The 8 October 2006 M_d 4.5 Cowlitz Chimneys Earthquake in Mount Rainier National Park

Renate Hartog,[1] Joan Gomberg,[2] Seth C. Moran,[3] Amy Wright,[1] and Karen L. Meagher[2]

INTRODUCTION

An M_d 4.5 earthquake located ~ 12 km east of Mount Rainier occurred on 8 October 2006 at 02:48 UTC (figure 1). Although not large enough to be damaging or of major tectonic significance, a summary description of the earthquake is warranted because of its proximity to Mount Rainier, and because earthquakes of $M_d \geq 4.5$ are relatively rare in this region. Previous events of $M_d \geq 4.5$ have occurred approximately once a decade within a radius of ~ 60 km from this mainshock, with the closest and most recent prior earthquake being an M_d 4.9 event located 46 km to the southwest in 1989. Magnitudes in this paper refer to the coda duration magnitude determined by the Pacific Northwest Seismic Network (PNSN) (Crosson 1972). We refer to the 2006 event as the "Cowlitz Chimneys" earthquake because it occurred beneath the Cowlitz Chimneys, a prominent ridge in Mount Rainier National Park.

This paper describes the mainshock's focal mechanism and its aftershock distribution. The inferred source mechanism, its ordinary aftershock sequence, and the lack of significant triggered seismicity near the volcanic edifice lead us to conclude that this was a regular tectonic crustal earthquake rather than one related to volcanic processes.

BACKGROUND

The Cowlitz Chimneys epicentral region lies within the Cascades mountain range, an active subduction-related volcanic arc. Seismologic, geologic, and GPS observations show the epicentral region to be in an area of compressive stress, resulting from subduction of the Juan de Fuca plate beneath the North American plate and large-scale rigid block rotation believed to be driven by motions and deformation well outside the region (*e.g.*, northward translation of the Sierra Nevada and Basin and Range extension). On a broad scale, rigid block models of McCaffrey *et al.* (2007) suggest that the Cowlitz Chimneys event lies in the center of a narrow block bounded by north-south- and northwest-southeast-trending faults. Relative slip vectors across these faults point toward the southwest (*i.e.*, east- and northeast-dipping thrusts) and suggest very modest velocities of a few mm/yr or less. Regional maximum and minimum compressive stresses estimated from focal mechanisms are nearly horizontal. East and west of Mount Rainier, maximum and minimum compressive stresses trend roughly north-south and east-west, respectively. Maximum compressive stresses rotate by about 27° and trend northwest in the St. Helens seismic zone (Ma *et al.* 1991; Giampiccolo *et al.* 1999).

Mount Rainier's edifice has negligible effect on the deformation field just kilometers from its flanks. Mount Rainier is about 500,000 years old (Lanphere and Sisson 1995) and erupted most recently in 1894, producing a light dusting of ash (Sisson *et al.* 2001, 113). Rainier seismicity consists of volcano-tectonic (VT) events that occur at a relatively constant rate of several per month above the completeness coda magnitude of ~ 0.1. These VT events are believed to be associated with magmatic-hydrothermal fluid circulation (Moran *et al.* 2000). More than half of the Rainier summit focal mechanisms indicate normal faulting, and the remainder reflect strike-slip faulting (Malone *et al.* 1991; Giampiccolo *et al.* 1999; Moran *et al.* 2000). In contrast, seismicity in the surrounding region reflects the compressive regional-scale tectonics (*i.e.,* reverse and strike-slip mechanisms).

The Cowlitz Chimneys earthquake sits within a discontinuous alignment of epicenters extending north-northwest from an eroded Pliocene volcano called Goat Rocks (figure 1). This alignment lies along the boundary of a large, buried, high-conductivity feature called the southern Washington Cascades conductor (Stanley *et al.* 1996). Several felt earthquakes have occurred in the vicinity of Goat Rocks, most notably an M_d 5.0 event on 28 May 1981. Two more prominent epicenter alignments are the north-northwest-south-southwest trending Mount St. Helens seismic zone (SHSZ) and broader, north-south-trending, western Rainier seismic zone (WRSZ) (Thompson 1989; Weaver *et al.* 1990). The most prominent is the SHSZ, where events as large as M_d 5.5 have occurred (Weaver and Smith 1983). Earthquakes within the WRSZ rupture en echelon faults oriented at oblique angles relative to the epicentral trend (Thompson and Qamar 1989; Malone *et al.* 1991; Stanley *et al.,* 1996; Moran *et al.* 1999). In the WRSZ fault-plane solutions are typically either strike-slip or reverse mechanisms, and the largest event was the M_d 4.9 event of 1989. The SHSZ and

1. Pacific Northwest Seismic Network, University of Washington, Department of Earth and Space Sciences
2. U.S. Geological Survey, University of Washington, Department of Earth and Space Sciences
3. U.S. Geological Survey, Cascade Volcano Observatory

doi: 10.1785/gssrl.79.2.186

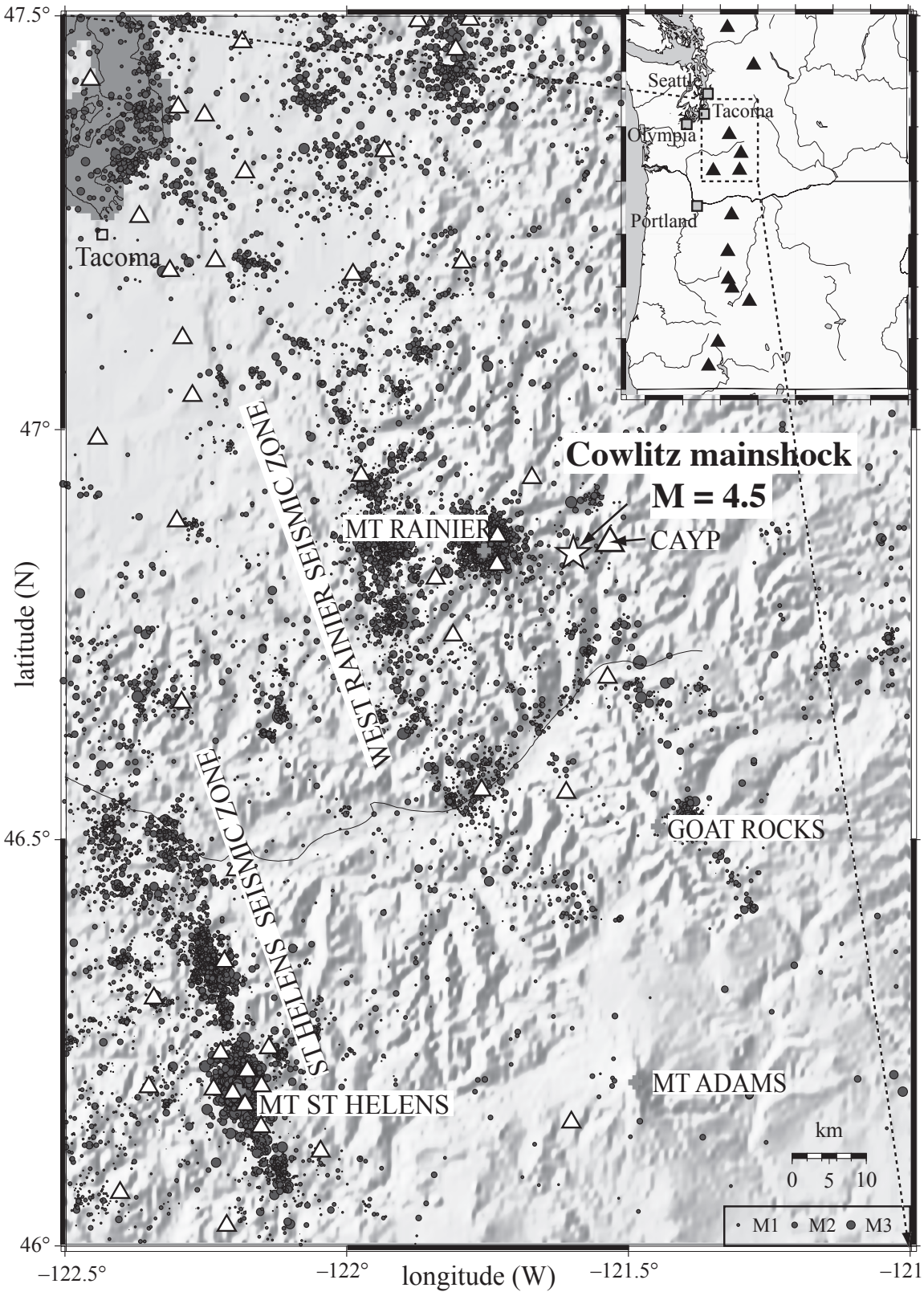

▲ **Figure 1.** Hillshade relief map derived from Digital Elevation Model (DEM; GTOPO3 interpolated to 1 arcsec) showing PNSN catalog locations of all earthquakes with $M_d > 0.0$ from 1 January 1969 up to 8 October 2006. The white star indicates the location of the $M_d = 4.5$ mainshock of 8 October 2006. Also labeled are the western Rainier seismic zone (WRSZ); the St. Helens seismic zone (SHSZ); volcanoes Mount Rainier, Mt. St. Helens, and Mt. Adams; the Goat Rocks volcanic center; and temporary seismic station CAYP. White triangles represent seismic stations.

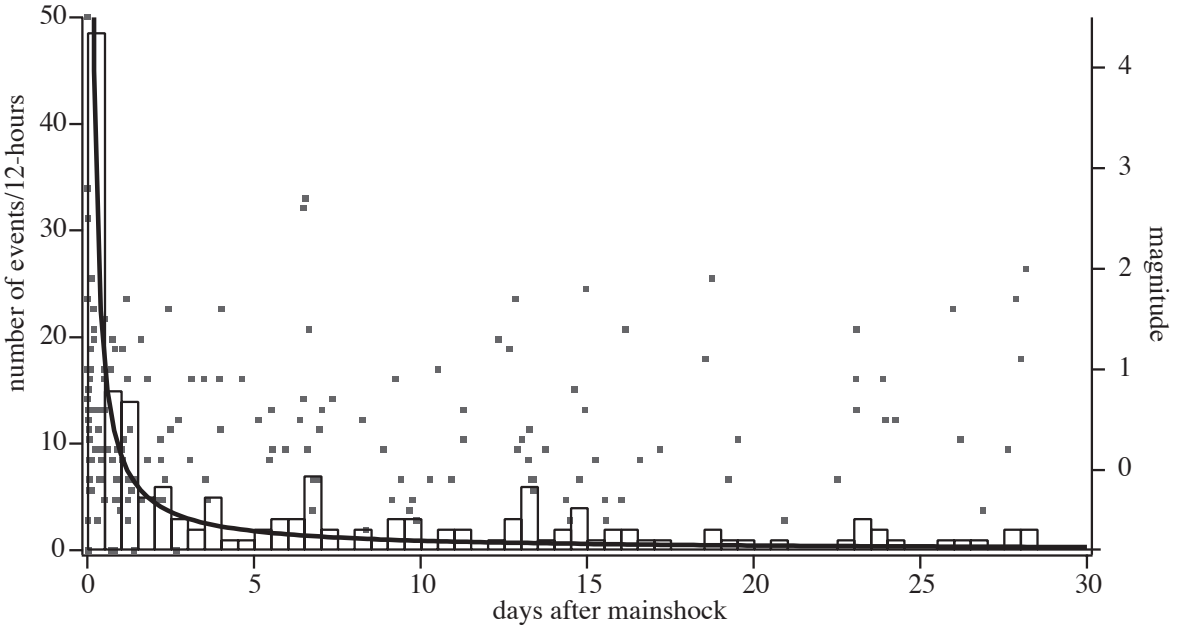

▲ **Figure 2.** Number of events per 12 hours (bars) and aftershock magnitude (gray squares) as a function of time in days since the origin time of the main shock. The black curve indicates number of aftershocks per 12 hours according to an Omori law function, $K/(c+t)$ with $K \sim 9$ and $c \sim 0.1$ and t time in days after mainshock.

WRSZ mark the eastern extent of the dense, igneous, Siletzia basement formation (Parsons *et al.* 2005 and references therein). The trend of the WRSZ does not correlate with the distribution of seismic velocities in tomographic images (Moran *et al.* 1999), nor is it directly related to volcanic processes occurring beneath Mount Rainier (Parsons *et al.* 2005).

THE COWLITZ CHIMNEYS EARTHQUAKE

The Cowlitz Chimneys mainshock-aftershock sequence occurred where PNSN station coverage is relatively sparse (figure 1), and most stations only have a vertical-component 1-Hz weak-motion sensor. The nearest PNSN site was 9 km from the mainshock's epicenter. Because no stations were within a focal-depth's distance and all nearby stations clipped, obscuring *S*-wave arrivals, the PNSN catalog depth of 3.8 km is not well-constrained. First-motion polarities fit best with an almost pure, thrust-fault focal mechanism where the two possible planes have strikes of 115° and 272° clockwise from N, dips of 65° and 27°, and rakes of 100° and 69°. Aftershock locations (below) suggest that the shallower, northeast-dipping plane is the true fault plane. The *P* axis is oriented north-northeast-south-southwest (azimuth is 198°, dip is 19°), consistent with the regional-scale compressive tectonics.

Even though the epicenter was located in a remote area of Mount Rainier National Park, 1,286 people in 198 ZIP Code areas filed online Community Internet Intensity Map reports, with the maximum intensity reported as MMI IV (light shaking and no damage). Such a response is consistent with the ShakeMap instrumental intensities and peak accelerations estimated at a few percent g within a few tens of km from the epicenter. ShakeMaps for the Pacific Northwest region can be found online at http://www.pnsn.org/shake/archive .

Aftershocks and Background Seismicity

The Cowlitz Chimneys mainshock had a rich aftershock sequence of 63 locatable earthquakes within the first 24 hours of the mainshock and about 200 aftershocks total from 8 October to 31 December 2006. The temporal behavior of the aftershock sequence agrees with the regional Pacific Northwest lore that shallow (depth < 30 km) mainshocks have significant aftershock sequences and deeper (depth > 30 km) mainshocks do not have many aftershocks. The paucity of pre-mainshock seismicity makes aftershock identification from the PNSN catalog straightforward. The smallest locatable aftershocks have magnitudes of ~ −0.8. The number of cataloged aftershocks appears to decay with time as in a standard aftershock sequence (figure 2). An Omori law function of the form $K/(c+t)^p$ describes the observed decay well. Here t is time since mainshock in days, empirical constants are $K = 9$, c is less than a few minutes, and $p \sim 1$. Sporadic increases in the number of aftershocks compared to the Omori law prediction plausibly correspond to secondary aftershocks, suggested by the occurrence of larger magnitude events at the time of the increases (figure 2).

The initial PNSN network locations of the aftershocks suggested an elongated aftershock pattern. Though most events clustered near the mainshock hypocenter, the pattern extended southeast and northwest. Aftershocks located as far as just north of the Mount Rainier summit (figure 3) caused speculation about whether a dike intrusion caused the linear pattern or whether the spatial distribution of stations used in locating the events caused an artificial pattern. To resolve this ambigu-

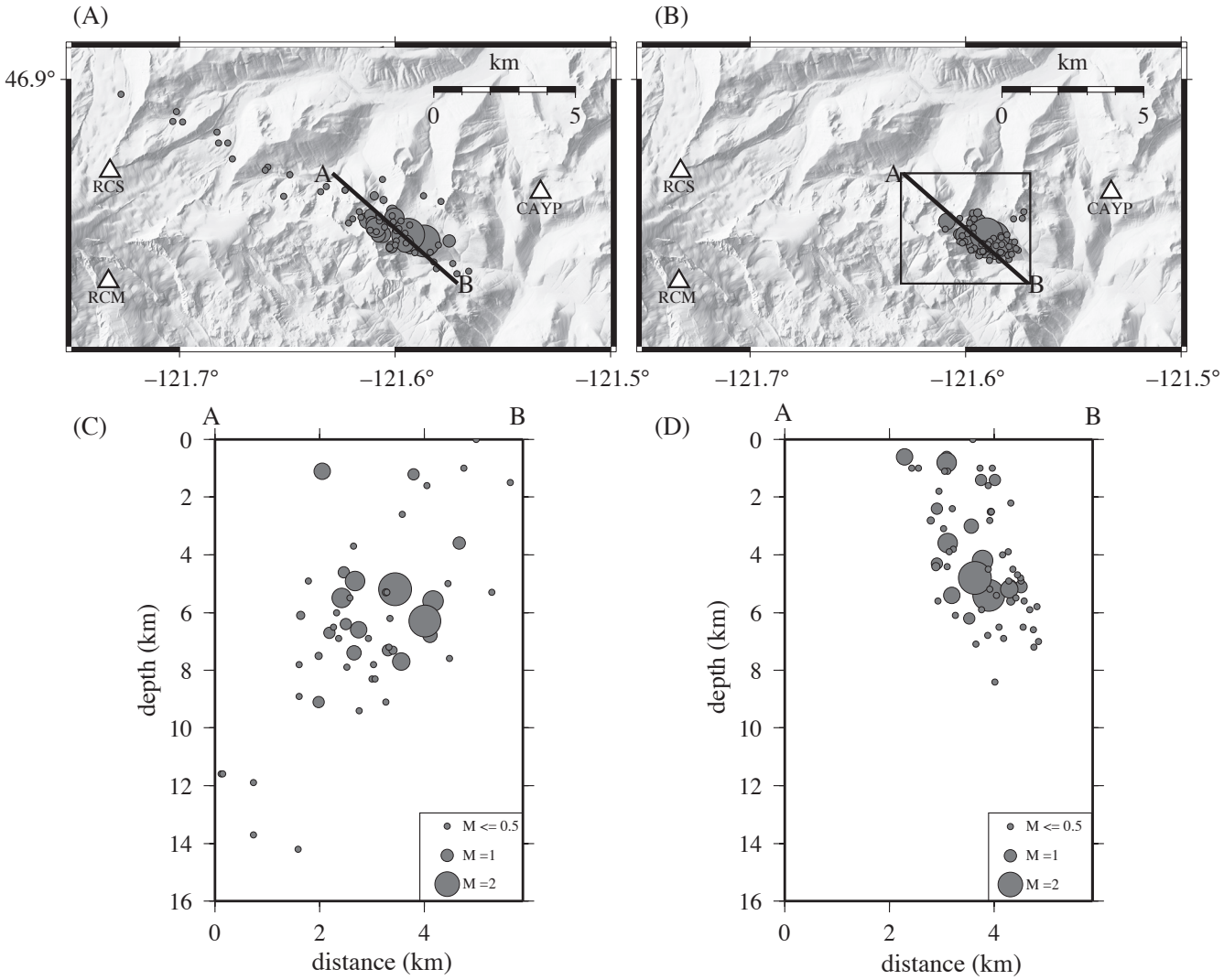

▲ **Figure 3.** Upper panel: Map views of 67 aftershock PNSN catalog locations obtained A) without CAYP picks, and B) with CAYP picks; locations (gray circles) are plotted on top of 1/3-s hillshade relief DEM and circles are scaled by magnitude. Triangles are temporary station CAYP and permanent stations RCS and RCM. The rectangular box in B outlines the area shown in figure 5A. Lower panel: depth cross-sections A-B showing the catalog locations obtained C) without CAYP picks and D) with CAYP picks.

ity, two portable three-component broadband stations recording with sample rates of 100 Hz were installed by the Cascades Volcano Observatory (CVO) within 24 hours of the mainshock, at distances of 5 km and 3.5 km from its epicenter. A week later the stations were removed due to inclement weather. Unfortunately the GPS clock of the closer station did not lock. Arrival times of 67 aftershocks were picked on records recorded by the other temporary station, named Cayuse Pass (CAYP). These arrival times significantly improved the locations of these 67 aftershocks as determined by our standard location program, yielding a much smaller spatial distribution of aftershocks (figure 3). Most location estimates (51) changed less than 2 km with the inclusion of CAYP picks; however, some locations (16) moved from 3 to 10 km. Initial locations of some smaller events were further northwest and deeper than locations that included CAYP picks. The addition of one well-placed temporary station reduces location error sufficiently to confirm that the initial elongate aftershock pattern was due to the spatial distribution of stations rather than a dike intrusion.

To study the seismicity pattern around Cowlitz Chimneys further, we relocated earthquakes from the area using the double-difference relocation program HypoDD (Waldhauser and Ellsworth 2000). We also included small events that occurred in the area prior to the mainshock, but that our standard processing routine may have mis-located. Using earthquakes occurring between 1990 and 2006 and eliminating events listed as explosions in the PNSN catalog yielded a total of 1,603 earthquakes in a region including the summit of Mount Rainier and the area to the east (figure 4). We did not limit our selection on the basis of location quality because good relative locations can be obtained even if the data are insufficient to obtain good absolute locations with traditional, single-event methods.

We converted our catalog arrival times to difference times using the preprocessing software ph2dt (Waldhauser 2001). The

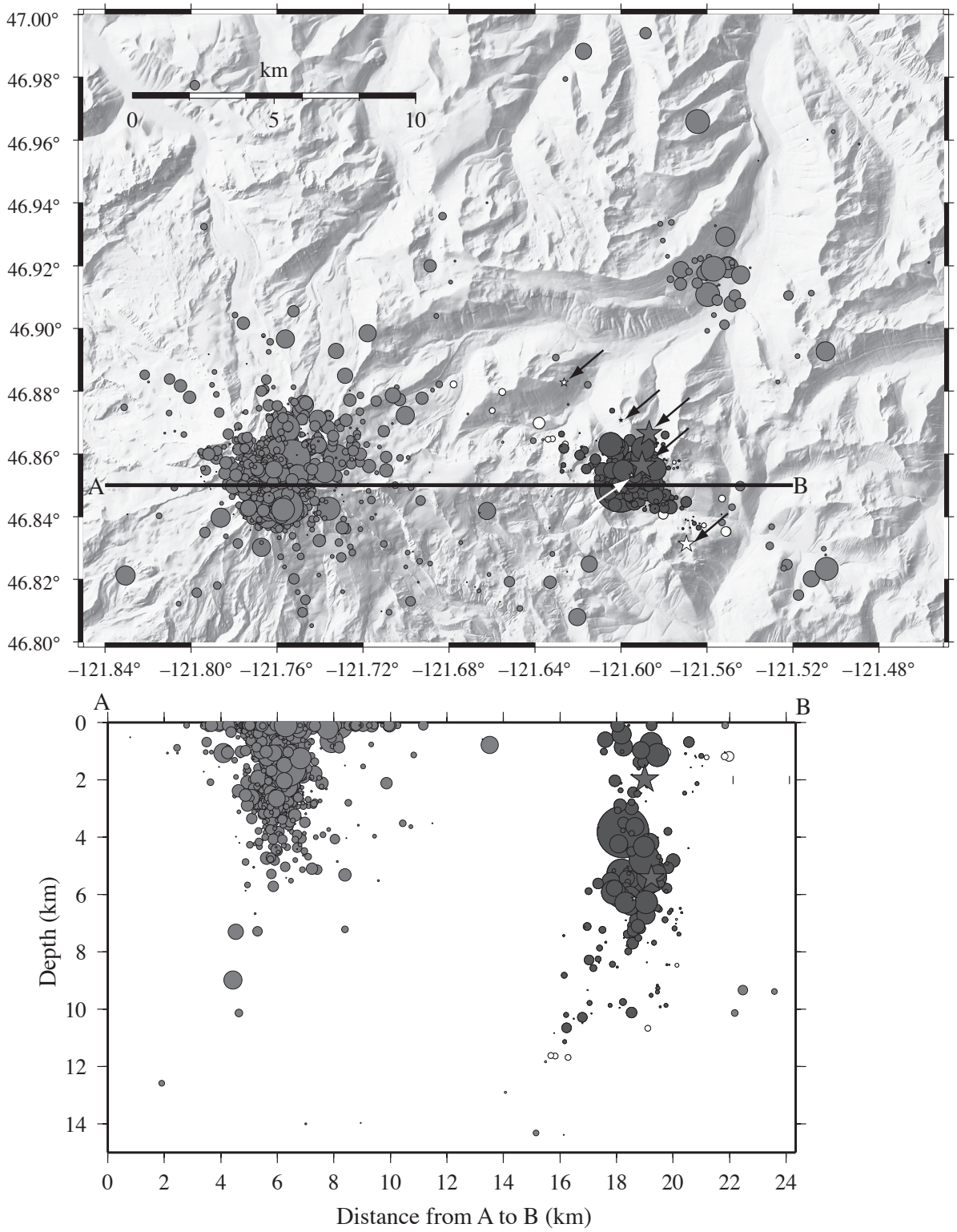

▲ **Figure 4.** Map view and cross-section showing catalog locations of 1,603 earthquakes that occurred between 1 January 1990 and 31 December 2006 and that were selected to be clustered with HypoDD. The depth cross-section only includes hypocenters within 2 km of A-B. Gray circles denote events that were not part of the Cowlitz Chimneys cluster (1,396 events), white circles were selected by HypoDD but not successfully relocated (29 events), and the dark gray circles denote events that were part of the cluster and successfully relocated (178 events, see figure 5). Circle size is proportional to event magnitude. Stars indicate events within the Cowlitz Chimneys cluster that occurred before the mainshock. Their size has been enlarged compared to the circles, and they are marked by arrows to aid with identification.

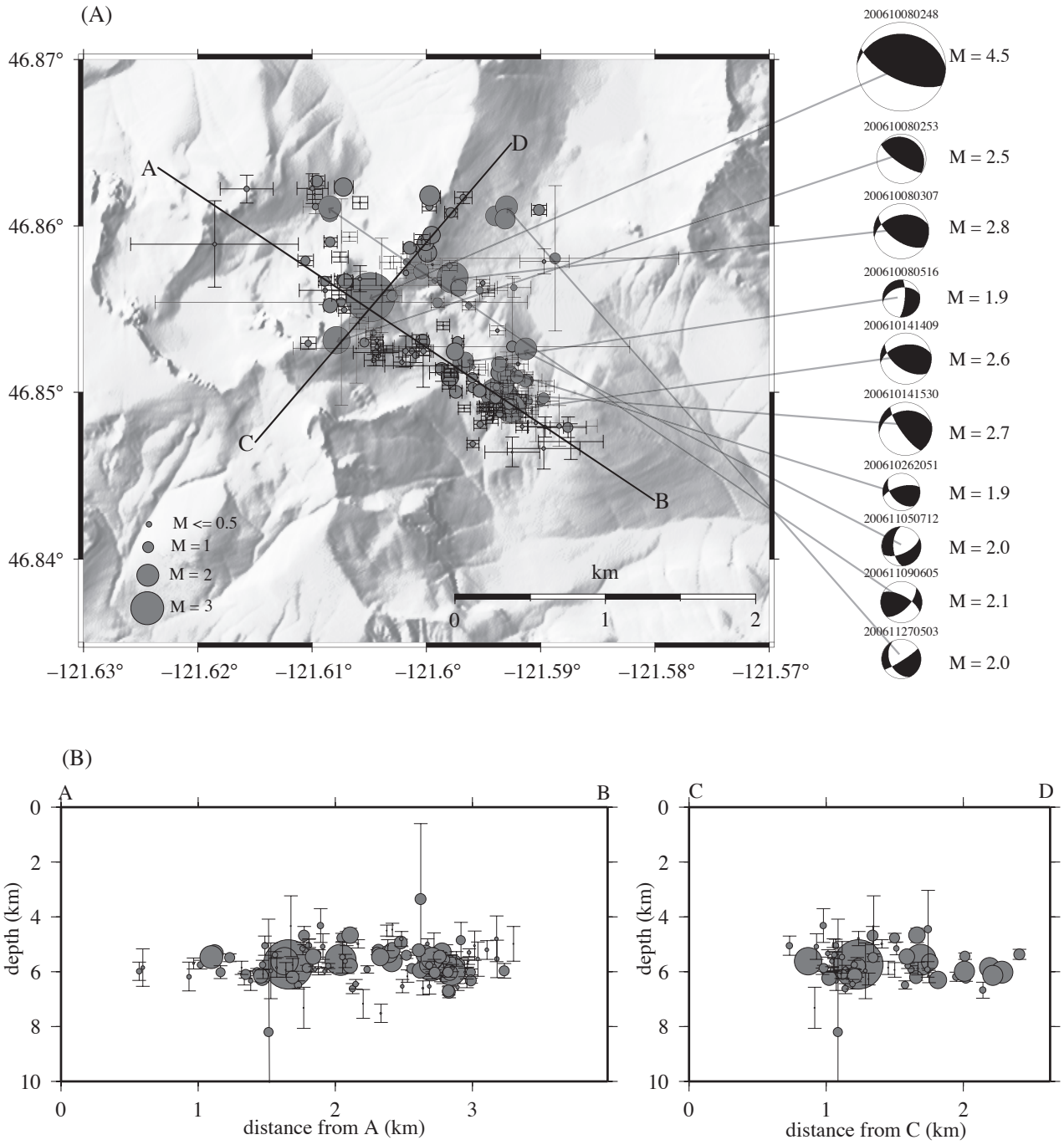

▲ **Figure 5.** (A) Map view of 178 earthquake locations and error bars in mainshock region as determined by HypoDD. Circles are scaled by magnitude. Focal mechanism of the mainshock and nine larger aftershocks are also shown. (B) Cross-sections A-B and C-D showing depth distribution of HypoDD locations with vertical error bars. Note that the horizontal exaggeration masks apparent dip of aftershock sequence.

average distance between event pairs was 2.8 km and 1.7 km for weakly (between 4 and 8 phase pairs in common) and strongly (8 or more phase pairs in common) linked events, respectively. We investigated various combinations of HypoDD parameters and ultimately chose a combination that counted the aftershocks farther from the mainshock as part of the Cowlitz Chimneys cluster. Our choice enabled HypoDD to calculate valid locations for most of the earthquakes in the cluster while obtaining a large variance reduction. We used the cluster centroid location as the starting point and required a minimum of four observations per event pair, a residual cut-off of six standard deviations (allows fairly large residuals to be retained in order to minimize the number of data discarded), and a maximum interevent distance of two km. Given these parameters, HypoDD split the 1,603 events into three large clusters and several small clusters containing five or fewer events. The largest cluster contains

events near Rainier's summit (1,234 events), the second largest cluster contains the Cowlitz Chimneys mainshock (207 events; all but seven are aftershocks), and a third cluster locating a bit north of Cowlitz Chimneys contains 35 events (figure 4). We found only six small pre-2006 events in the PNSN catalog near the Cowlitz Chimneys event (marked by arrows in figure 4). The Cowlitz Chimneys earthquake is therefore the first (recorded) significant event in this part of the national park. The northern cluster includes only small events ($-0.5 \le M_d \le 2.2$). A search of the catalog further back in time reveals that the first recorded activity in this northern cluster occurred in April 1975 with an M_d 3.9 felt event on 18 April 1975, which was preceded by two smaller events on 11 and 15 April with M_d 2.1 and 2.3, respectively. Only two events with $M_d \ge 2.0$ have occurred there since.

HypoDD offers the choice of using a robust singular value decomposition (SVD) and a more approximate conjugate-gradients method (Paige and Saunders 1982) to solve the linear double-difference equations. We relocate only the Cowlitz Chimneys cluster, because its small size allows use of the SVD method. The SVD method provides formal errors that indicate the uncertainty of the new earthquake locations. HypoDD was able to locate 178 of the 207 events with a variance reduction of 99% and a reduction of the average root mean square of the difference times from 0.153 s to 0.0179 s (figure 5).

HypoDD significantly reduced hypocenter scatter compared with the standard method in which each location is determined absolutely and independently. In particular, whereas the earthquakes appear distributed over a large depth-range when located with the traditional location method (figure 4), the majority of HypoDD locations lie between 4 and 8 km depth (figure 5). The spatial pattern of hypocenters is well-constrained and does not vary significantly with slightly different HypoDD parameters. However, the absolute location of the cluster is less certain. In particular, if we use the catalog locations rather than the cluster centroid as starting locations, the whole cluster shifts ~ 250 m to the west and is located slightly shallower (~ 200 m). If we use the more approximate conjugate gradients method to solve the set of equations rather than the SVD method, the cluster shifts ~ 750 m to the south-southwest. The CAYP picks help constrain the absolute location of the cluster because if we do not include the CAYP picks, the whole cluster shifts ~ 1 km to the west-northwest and 1 km deeper; the relative spatial pattern of the earthquakes is retrieved even without the CAYP picks. The HypoDD aftershock locations spread over an area of ≈ 2 km^2, consistent with the rupture area expected for an **M** 4.5 rupture (Kanamori and Anderson 1975; Abercrombie 1995), on the shallowly dipping plane inferred from the mainshock focal mechanism. Focal mechanisms for nine larger aftershocks ($M_d \ge 1.9$) were determined with FPFIT (Reasenberg and Oppenheimer 1985), using the HypoDD locations, the PNSN velocity model for the Cascade region, and PNSN catalog polarities (figure 5). Seven of these focal mechanisms are consistent with reverse faulting on a shallowly dipping N-NE-dipping fault. In general, the *P* axes vary less between focal mechanisms than the *T* axes, and the orientations of the *P* axes tend to be better constrained as alternate focal mechanisms for several aftershocks have similar *P*-axis orientations but variable *T*-axis orientations.

Triggering at Mount Rainier?

The passage of seismic surface waves generated by the 2002 M_W 7.9 Denali Fault earthquake (DFE) in Alaska triggered small earthquakes at Mount Rainier (Prejean *et al.* 2004). It is plausible that the shaking from a nearby earthquake would trigger earthquakes in the volcano as well. Several earthquakes near or within the Rainier summit occurred during the first four hours after the Cowlitz Chimneys mainshock, which is suggestive of triggering given the infrequent occurrence of VT events but not conclusive. In comparison, more than twice this number of events was triggered in the same time interval in association with the DFE.

The exact mechanism responsible for dynamic earthquake triggering is still unknown. Peak velocities, known to be proxies for strains, are one measure that may serve as a triggering criterion. The DFE peak velocities at nearby strong-motion station LON were ~ 1.0 cm/s, roughly twice the peak velocities recorded for the Cowlitz Chimneys mainshock. However, in addition to higher peak velocities, DFE waves had much lower dominant frequencies (~ 0.05 Hz) than those of the local Cowlitz Chimneys event (~ 10 Hz). A more detailed study, beyond the scope of this paper, might determine which characteristics of wavefields are most effective in triggering earthquakes at Mount Rainier.

DISCUSSION AND CONCLUSIONS

Although intriguing lineations appear in the digital elevation image and on the geologic map (Fiske *et al.* 1964), no identified fault coincides with the location of the mainshock and aftershocks (T. Sisson, personal communication 2007). The aftershocks do, however, lie within a coherent high-velocity feature in a 3D tomographic model (Moran *et al.* 1999). Perhaps these earthquakes are occurring preferentially in more competent rock. The focal mechanism for the mainshock, the spatial distribution of aftershocks, and focal mechanisms of the larger aftershocks all indicate that the event occurred on a subhorizontal reverse fault at about 6 km depth. This reverse fault and the implied orientation of the principal axes (maximum compressive stress almost horizontal and oriented NNE-SSW) are consistent with the regional-scale compressive tectonics (McCaffrey *et al.* 2007; Ma *et al.* 1991; Giampiccolo *et al.* 1999). In addition, the number of aftershocks as a function of time since the mainshock is typical of crustal earthquakes. We therefore conclude that the Cowlitz Chimneys earthquake was due to the regional tectonic stress field and not directly related to volcanic processes at Mount Rainier. The shaking of the volcanic edifice due to the Cowlitz Chimneys event may have triggered a few small earthquakes near the summit of the volcano; however, the number of summit quakes was too small to rule out that they would have occurred regardless of the Cowlitz Chimneys event.

The Cowlitz Chimneys earthquake occurred in a small area where the PNSN had not previously located earthquakes

and where the network is sparse. To study earthquakes like this one and their aftershocks effectively, quick deployment of high-quality instruments in the aftershock region is critical. One strategically placed seismometer can significantly improve the accuracy of aftershock locations. Furthermore, in a relative earthquake location scheme such as the double-difference algorithm, the additional constraints provided by temporary stations also improve location accuracy for events that occurred before the stations were deployed.

ACKNOWLEDGMENTS

We thank Dave Ueberoff, Superintendent of Mount Rainier National Park, for rapidly granting permission for the installation of two temporary seismometers within the park, and several Mount Rainier staff members, particularly Peter Maggio and Geoff Walker, for helping us access parts of the park that had been closed off for the winter. We thank Susan Bilek, Heather DeShon, Stephen Malone, and James Vallance for reviews that significantly improved the original manuscript. Figures were partly made using the Generic Mapping Tool (Wessel and Smith 1998). This research was funded, in part, by the U.S. Geological Survey Cooperative Agreement 07HQAG0011 and by funding from the State of Washington to support activities of the Pacific Northwest Seismic Network.

REFERENCES

Abercrombie, R. E. (1995). Earthquake source scaling relationships from -1 to 5 ML using seismograms recorded at 2.5-km depth. *Journal of Geophysical Research* **100** (B12), 24,015–24,036.

Crosson, R. S. (1972). Small earthquakes, structure, and tectonics of the Puget Sound region. *Bulletin of the Seismological Society of America* **62** (5), 1,133–1,171.

Fiske, R. S., C. A. Hopson, and A. C. Waters (1964). Geologic Map and Section of Mount Rainier National Park Washington. Miscellaneous Geologic Investigations, MAP I-432, USGS.

Giampiccolo, E., C. Musumeci, S. D. Malone, S. Gresta, and E. Privitera (1999). Seismicity and stress-tensor inversion in the central Washington Cascade Mountains. *Bulletin of the Seismological Society of America* **89** (3), 811–821.

Kanamori, H., and D. L. Anderson (1975). Theoretical basis of some empirical relations in seismology. *Bulletin of the Seismological Society of America* **65** (5), 1,073–1,095.

Lanphere, M. A., and T. W. Sisson (1995). K-Ar ages of Mount Rainier volcanics. *EOS, Transactions, American Geophysical Union* **76** (46), 651.

Ma, L., R. S. Crosson, and R. S. Ludwin (1991). *Focal Mechanisms of Western Washington Earthquakes and Their Relationship to Regional Tectonic Forces*. USGS Open-File Report OF-91-0441-D, 38 pps.

Malone, S. D., A. Qamar, and C. Jonientz-Trisler (1991). Recent seismicity studies at Mount Rainier, Washington. *Seismological Research Letters* **62** (1), 25.

McCaffrey, R., A. I. Qamar, R. W. King, R. Wells, G. Khazaradze, C. A. Williams, C. W. Stevens, J. J. Vollick, and P. C. Zwick (2007). Fault locking, block rotation and crustal deformation in the Pacific Northwest. *Geophysical Journal International* **169** (3), 1,315–1,340.

Moran, S. C., J. M. Lees, and S. D. Malone (1999). *P* wave crustal velocity structure in the greater Mount Rainier area from local earthquake tomography. *Journal of Geophysical Research* **104** (B5), 10,775–10,786.

Moran, S. C., D. R. Zimbelman, and S. D. Malone (2000). A model for the magmatic–hydrothermal system at Mount Rainier, Washington, from seismic and geochemical observations. *Bulletin of Volcanology* **61**, 425–436.

Paige, C. C., and M. A. Saunders (1982). LSQR: Sparse linear equations and least squares problems. *ACM Transactions on Mathematical Software* **8** (2), 195–209.

Parsons, T., R. J. Blakely, T. M. Brocher, N. I. Christensen, M. A. Fisher, E. Flueh, F. Kilbride, J. H. Luetgert, K. Miller, U. S. ten Brink, A. M. Trehu, and R. E. Wells (2005). *Crustal Structure of the Cascadia Fore Arc of Washington*. USGS Professional Paper 1661-D, 45 pps.

Prejean, S. G., D. P. Hill, E. E. Brodsky, S. E. Hough, M. J. S. Johnston, S. D. Malone, D. H. Oppenheimer, A. M. Pitt, and K. B. Richards-Dinger (2004). Remotely triggered seismicity on the United States West Coast following the Mw 7.9 Denali Fault earthquake. *Bulletin of the Seismological Society of America* **94** (6B), S348–S359.

Reasenberg, P., and D. Oppenheimer (1985). *FPFIT, FPPLOT AND FPPAGE: Fortran Computer Programs for Calculating and Displaying Earthquake Fault-plane Solutions*. USGS Open-File Report, OFR 85-739.

Sisson, T. W., J. W. Vallance, and P. T. Pringle (2001). Progress made in understanding Mount Rainier's hazards. *Eos, Transactions, American Geophysical Union* **82** (9), 118–120.

Stanley, W. D., S. Y. Johnson, A. I. Qamar, C. S. Weaver, and J. M. Williams (1996). Tectonics and seismicity of the southern Washington Cascade Range. *Bulletin of the Seismological Society of America* **86** (1), Part A, 1–18.

Thompson, K. I. (1989). Seismicity of Mt. Rainier: A detailed study of events to the west of the mountain and their tectonic significance. Master's thesis, University of Washington.

Thompson, K. I., and A. Qamar (1989). The seismicity of Mount Rainier, Washington. *Seismological Research Letters* **60** (1), 31.

Waldhauser, F., and W. L. Ellsworth (2000). A double-difference earthquake location algorithm: Method and application to the northern Hayward fault. *Bulletin of the Seismological Society of America* **90**, 1,353–1,368.

Waldhauser, F. (2001). HypoDD–A program to compute double-difference hypocenter locations. Online USGS Open-File Report, OFR 01-113.

Weaver, C. S., and S. W. Smith (1983). Regional tectonic and earthquake hazard implications of a crustal fault zone in southwestern Washington. *Journal of Geophysical Research* **88** (B12), 10,371–10,383.

Weaver, C. S., R. D. Norris, and C. Jonientz-Trisler (1990). Results of seismological monitoring in the Cascade Range, 1962–1989; earthquakes, eruptions, avalanches, and other curiosities. *Geoscience Canada* **17** (3), 158–162.

Wessel, P., and W. H. F. Smith (1998). New, improved version of Generic Mapping Tools released. *Eos, Transactions, American Geophysical Union* **79** (47), 579.

Pacific Northwest Seismic Network
University of Washington
Department of Earth and Space Sciences
Box 351310
Seattle, WA 98195 USA
renate@ess.washington.edu
(R. H.)